PERGAMON

International Journal of Heat and Mass Transfer 46 (2003) 513–522

International Journal of HEAT and MASS TRANSFER

www.elsevier.com/locate/ijhmt

Nucleation site interaction in pool boiling on the artificial surface

Lei Zhang *, Masahiro Shoji

Department of Mechanical Engineering, School of Engineering, The University of Tokyo, 7-3-1 Hongo, Bunkyo-ku, 113-8656 Tokyo, Japan

Received 11 March 2002; received in revised form 21 June 2002

Abstract

The present work aims at studying the physical mechanisms of nucleation site interaction in pool boiling. A series of experiments have been carried out to investigate the average bubble departure frequency $\overline{f_d}$ of two artificial cavities on the thin silicon surface for different dimensionless cavity spacing $S/\overline{D_b}$, that is the ratio of the cavity spacing to the average bubble departure diameter. Based on the comprehensive observation and analysis, three significant effect factors of nucleation site interaction are found out: Ⓐ hydrodynamic interaction between bubbles; Ⓑ thermal interaction between nucleation sites; Ⓒ horizontal and declining bubble coalescences. The intensity, competition and dominance relations of these three factors determine four different interaction regions: 'I' region ($S/\overline{D_b} > 3$), 'H' region ($2 < S/\overline{D_b} \leqslant 3$), 'H + T' region ($1.5 < S/\overline{D_b} \leqslant 2$) and 'H + T + C' region ($S/\overline{D_b} \leqslant 1.5$). In the 'I' region, the bubble departure frequency is similar to that in the single cavity condition as a result of the negligible effect of all the three factors. For the 'H' region, the stronger influence of factor Ⓐ results in a higher bubble departure frequency. Within the 'H + T' region, the co-existence and competition relation occurs between factors Ⓐ and Ⓑ. The dominance of factor Ⓑ causes the lower bubble departure frequency. As for the 'H + T + C' region, although all the three factors are strong and compete simultaneously, the promotive effect becomes dominant finally and the bubble departure frequency increases again. Through the present study, some essential aspects of the nucleation site interaction in pool boiling have been revealed, which is significant for better understanding the boiling mechanisms.

1. Introduction

Nucleation boiling has been extensively utilized in industry because it is one of the most efficient heat transfer modes, particularly in high energy density systems such as nuclear reactor power plants, electronics packaging and the like. In the past several decades, much effort has been directed toward determining the interrelationship between heat flux and surface superheat for a particular material, with less research being focused on understanding the nucleate boiling mechanisms [1], especially the nucleation site interaction mechanisms.

The relation between the bubble behavior and the dimensionless cavity spacing $S/\overline{D_b}$ has been studied experimentally by several authors in recent years. Chekanov [2] performed the earliest experiments to investigate the interaction of two artificial nucleation sites, which were created by two heated copper rods that were placed in contact with a permalloy plate covered with water. Experimental results stated that the elapsed time between bubble departures at neighboring nucleation sites was random and possessed a Gamma distribution. The relation between the shape parameter of the Gamma distribution γ and dimensionless separation distance $S/\overline{D_b}$ stated that for $S/\overline{D_b} \leqslant 3$, the formation of a bubble at one nucleation site inhibited the formation of a vapor bubble at the other nucleation site. While for $S/\overline{D_b} > 3$, the growth of a bubble on one nucleation site promoted the growth of a bubble on the other. When $S/\overline{D_b} \gg 3$,

* Corresponding author. Fax: +81-3-5841-6408.
E-mail address: zhang@photon.t.u-tokyo.ac.jp (L. Zhang).

0017-9310/03/$ - see front matter © 2002 Elsevier Science Ltd. All rights reserved.
PII: S0017-9310(02)00291-0

Nomenclature

A	laser-heated area, m^2
C	correlation function
C_D	drag force coefficient
D	bubble diameter, m
$\overline{D_b}$	average bubble departure diameter, m
d	cavity diameter, m
F_B	buoyancy force, N
F_σ	surface tension force, N
F_i	inertia force, N
F_d	drag force, N
f_d	bubble departure frequency, Hz
$\overline{f_d}$	average bubble departure frequency, Hz
g	gravitational acceleration, m/s^2
H	cavity depth, m
h	liquid convective heat transfer coefficient, $W/m^2\,K$
h_0	liquid convective heat transfer coefficient in single cavity condition, $W/m^2\,K$
h_{fg}	latent heat of evaporation of liquid, J/kg
n	total sampling number of temperature fluctuation
Q_{laser}	heat rate of laser irradiation, W
Q_{bubble}	heat rate removed by bubbles, W
Q_{loss}	heat rate dissipated by lateral heat conduction around laser irradiation area, W
q^*_{ap}	apparent heat flux of laser irradiation, $q^*_{ap} = Q_{laser}/A$, W/m^2
R	correlation coefficient
r	standard deviation
r_{laser}	radius of laser irradiation area, m
S	cavity spacing, m
ds/dt	bubble center velocity, m/s
t	time, s
T	transient temperature at a certain point on the surface, °C
$\overline{T}$	average temperature at a certain point on the surface, °C
$\overline{T_w}$	average surface temperature within the laser irradiation area, °C
T_f	liquid temperature, °C
V	bubble volume, m^3
V_b	bubble departure volume, m^3
v_w	average impressed velocity of the liquid wake, m/s
x	distance along a scan line within the laser-heated region, m
Δx	distance between two selected points used to calculate the heat loss, m

Greek symbols

ρ_l	liquid density, kg/m^3
ρ_v	vapor density, kg/m^3
σ	surface tension, N/m
ξ	fraction of liquid accompanying a growing bubble ($\xi = 11/16$)
θ	contact angle
λ	thermal conductivity of heated wall, W/m K
δ	thickness of heated wall, m

Subscripts

c	cavity
i	sampling number of temperature fluctuation
j	point around the cavity

there were no interactions. Calka and Judd [3] investigated the interaction phenomena occurring at adjacent nucleation sites during saturated boiling of dichloromethane and analyzed the experimental results by the similar method to that of Chekanov. From the results of the shape parameter γ for different $S/\overline{D_b}$, it was concluded that the interaction was promotive for $S/\overline{D_b} \leqslant 1$ while inhibitive for $1 < S/\overline{D_b} \leqslant 3$. When $S/\overline{D_b} > 3$, no interaction was detected. Gjerkeš and Golobič [4] studied the influence of decreasing the distance between artificially activated nucleation sites and a naturally activated nucleation site on their activity. The results of measurements indicated that the nucleation sites exerted an effect on each other. When the nucleation site spacing was reduced, the individual and total activity of the nucleation sites was reduced. At very small spacing, deactivation of a weaker, less-active nucleation site might occur. Bhavnani et al. [5] studied the bubble size and latent heat contribution for different cavity spacing and heat flux on the silicon wafer, which was immersed in FC-72. They found that the bubble departure diameter and latent heat distribution were highest for the triple-spaced surface while with the decrease of cavity spacing, latent heat distribution became lower. However, almost all the above conclusions are limited to the direct description and simple deduction of experimental phenomena, and lack of deep research of the essential interaction mechanisms. This problem is the topic of consideration in the present paper.

As we know, the boiling research includes three aspects: liquid, interface and heated wall (shown in Fig. 1). In the liquid side, the hydrodynamic interaction dominates the bubble behaviors, which can be further divided into hydrodynamic interaction between bubble and liquid bulk (interaction 1) and hydrodynamic interaction between bubbles (interaction 2). For the heated wall, the

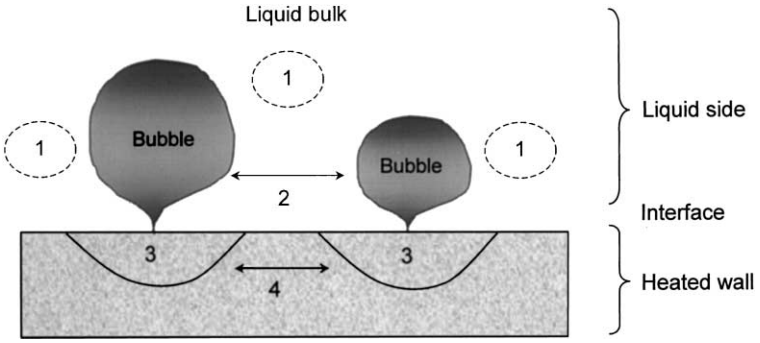

Fig. 1. Schematic diagram showing the effect factors of nucleation site interaction (1: Hydrodynamic interaction between bubble and liquid bulk. 2: Hydrodynamic interaction between bubbles. 3: Thermal interaction between nucleation site and heated wall. 4: Thermal interaction between nucleation sites).

thermal interaction rules the temperature distribution, which also includes two aspects: thermal interaction between nucleation site and heated wall (interaction 3) and thermal interaction between nucleation sites (interaction 4). Furthermore, interactions 1 and 3 can be found in single cavity and multiple cavities conditions, while interactions 2 and 4 only exist in the multiple cavities conditions. Although some researchers have studied the thermal interaction between nucleation site and heated wall (interaction 3) by experiments or simulations, the thermal interaction between nucleation sites (interaction 4) and the relation between thermal interaction and bubble behaviors have never been investigated [6–9].

On the other hand, the surface characteristics (roughness, aging, wettability) of the interface, which have dragged the boiling research into the biggest dilemma, have significant effect on the active nucleation site density and heat transfer characteristics. The active nucleation site density, however, can be easily controlled through applying the artificial boiling surfaces with one or two cavities. Although the cavity diameter and the cavity depth also have some influence on the bubble behaviors, the corresponding experimental results will be stated in another paper. Accordingly, the present work only focuses on the investigation of hydrodynamic interaction and thermal interaction, while the effect of surface characteristics, including the influence of cavity diameter and cavity depth, have been neglected by applying the same size for all the artificial cavities.

In the present research, a series of experiments are performed to study the relation between bubble departure frequency and cavity spacing on the thin silicon artificial surface. Three significant effect factors of nucleation site interaction are found out and four interaction regions are proposed according to the evolution of interaction mechanisms. The theory of nucleation site interaction mechanisms can be verified satisfactorily by the present experimental results.

2. Experimental setup

2.1. Heated surface with artificial cavities

In this study, single cavity and twin cavities with different spacing were tested as nucleation sites. They were respectively manufactured on or around the center of a 0.2 mm thick 15 mm diameter silicon plate. The treated cavities were all cylinders with a diameter $d = 10$ μm and a depth $H = 80$ μm (see Fig. 2(a)). The spacing of twin cavities was designed to be 1, 2, 3, 4, 6 and 8 mm.

2.2. Apparatus

A series of experiments have been conducted to study the nucleation site interaction in pool boiling on the artificial surface. An overview of the experimental apparatus is shown in Fig. 3. In the experiments, the silicon plate with the artificial cavities was set inside the boiling chamber filled with saturated distilled water. The vicinity of the manufactured cavities was heated by Nd-YAG laser irradiation from the bottom of the silicon plate. The bottom surface of the silicon plate was black oxide finished to increase absorptivity of the input laser. A simplified illustration of vicinity of two cavities is shown in Fig. 2(b) and (c). The power of Nd-YAG laser was controlled to vary the heat input to the silicon plate surface. The temperature fluctuation beneath and around the cavities was measured by radiation thermometer with a spatial resolution 120 μm, a temperature resolution 0.08 K and a time resolution 3.0 ms. In this way, it was possible to measure temperature–time series of cavity vicinity without any physical contact to the silicon plate surface. For the visual observations, a high-speed video with the rate of 1297 frames/s was used to record the corresponding bubble behaviors.

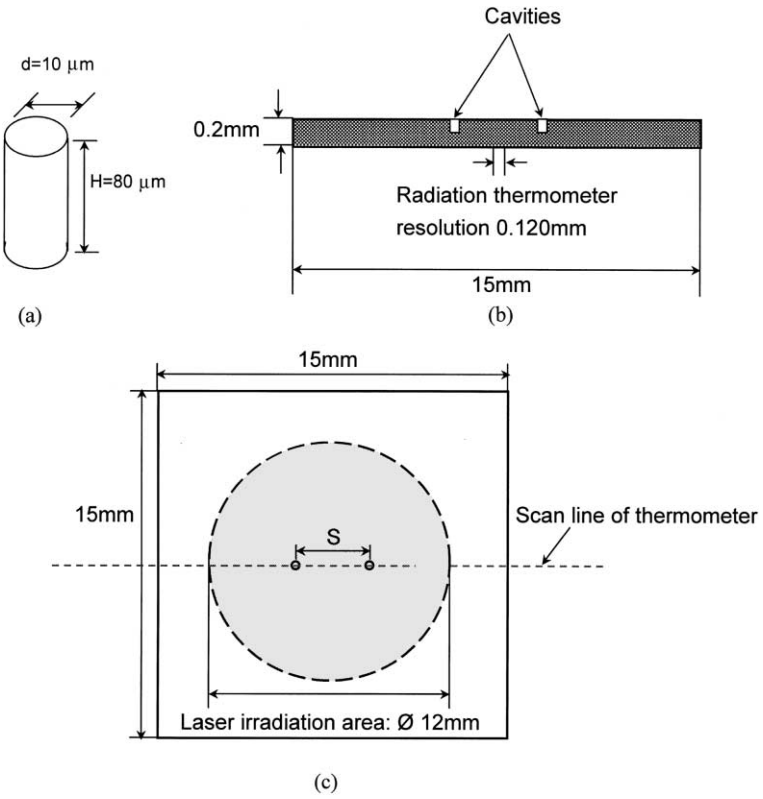

Fig. 2. Illustration of cavity and heated surface: (a) cavity size; (b) sectional view of heated surface; (c) vertical view of heated surface (S is designed to be 1, 2, 3, 4, 6 and 8 mm).

3. Results and discussion

3.1. Effect of cavity spacing on bubble departure frequency

In the experiments, the interest is aroused by the fact that the average bubble departure frequency is greatly influenced by the variation of $S/\overline{D_b}$ (see Fig. 4). The average bubble departure frequency is lowest for $S/\overline{D_b} > 3$, which is similar to that of the single cavity surface. With decreasing the cavity spacing, the average bubble departure frequency firstly increases within the region of $2 < S/\overline{D_b} \leqslant 3$, then decreases as $1.5 < S/\overline{D_b} \leqslant 2$ and finally increases again in the range of $S/\overline{D_b} \leqslant 1.5$.

3.2. Effect factors of nucleation site interaction

Although the present study only focuses on the hydrodynamic interaction and thermal interaction, the hydrodynamic interaction between bubbles can be further divided into two aspects: interaction between bubbles transferred by the liquid and direct interaction between bubbles, which is also called bubble coalescence. Through the observation of bubble behaviors it is found that the occurrence of bubble coalescence also has great influences upon the bubble departure frequency. Therefore, in the present research, the effect factors of nucleation site interaction are classified into three aspects: hydrodynamic interaction, thermal interaction and bubble coalescence, where the hydrodynamic interaction is specially defined as the interaction transferred by the liquid without bubble coalescence.

3.2.1. Hydrodynamic interaction

Both two kinds of hydrodynamic interactions (interactions 1 and 2) are induced by the bubble growth and departure. Conversely, the occurrence of these hydrodynamic interactions will influence the liquid wake velocity around the bubbles, which brings some effects on the bubble behaviors.

Zhang and Shoji [10] have investigated the overall force balance acting on the bubble in the air–water isothermal system. For the vapor bubble, the theoretical description of forces can be stated as follows:

(a) *Buoyancy force*

$$F_B = V(\rho_l - \rho_v)g \tag{1}$$

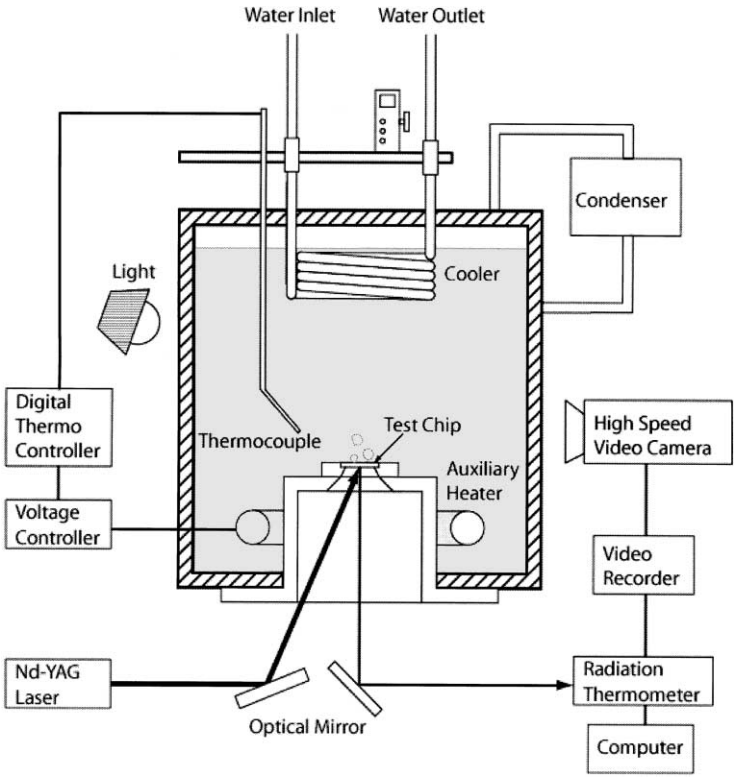

Fig. 3. Schematic view of experimental apparatus.

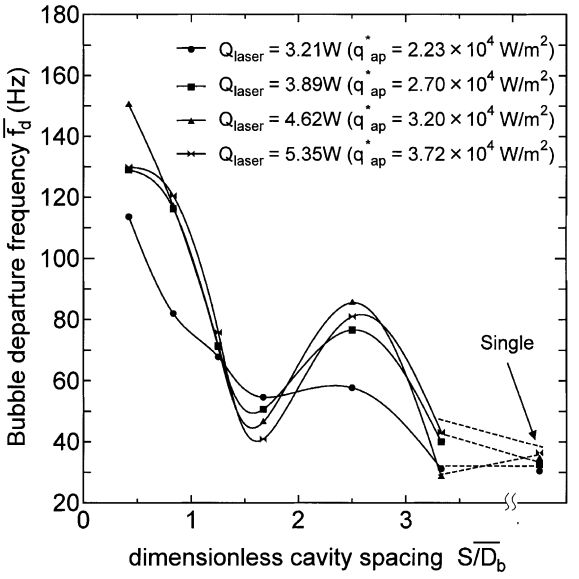

Fig. 4. Average bubble departure frequency $\overline{f_d}$ for different $S/\overline{D_b}$ and laser power Q_{laser}.

(b) *Surface tension force*

$$F_\sigma = \pi D \sigma \sin\theta \tag{2}$$

(c) *Added mass inertia force*

$$F_i = (\rho_v + \xi\rho_l)\frac{d}{dt}\left(V\frac{ds}{dt}\right) \tag{3}$$

(d) *Drag force*

$$F_d = \frac{1}{2}\rho_l\frac{\pi}{4}D^2 C_D\left(\frac{ds}{dt} - \upsilon_w\right)\left|\frac{ds}{dt} - \upsilon_w\right| \tag{4}$$

The force balance of the bubble at the departure moment can be described as follows:

$$F_B = F_\sigma + F_i + F_d \tag{5}$$

The stronger the hydrodynamic interaction, the larger the liquid wake velocity υ_w is and the smaller the drag force is. Therefore, the hydrodynamic interaction is promotive for the bubble departure.

In order to evaluate the intensity of the hydrodynamic interaction quantitatively, the convective heat transfer coefficient is calculated as

$$h = \frac{Q_{laser} - Q_{bubble} - Q_{loss}}{(\overline{T_w} - T_f)A} \tag{6}$$

where Q_{bubble} is the heat rate removed by the bubble generation and is calculated as

$$Q_{\text{bubble}} = V_b \rho_v h_{fg} f_d \tag{7}$$

Q_{loss} is the heat loss dissipated by the lateral heat conduction around the laser-heated region and is computed as

$$Q_{\text{loss}} = \lambda \frac{(\overline{T_{\text{in}}} - \overline{T_{\text{out}}})}{\Delta x} 2\pi r_{\text{laser}} \delta \tag{8}$$

where $\overline{T_{\text{in}}}$ is the average temperature of a point on the scan line inside the laser irradiation area and $\overline{T_{\text{out}}}$ is the average temperature of a point on the scan line outside the laser irradiation area. These two selected points are approximately symmetric with respect to the boundary line of the laser irradiation area and the distance between these two points is equal to 1.2 mm. In the single cavity condition, h can be looked as the evaluation of interaction 1 and defined as h_0, since only the hydrodynamic interaction between bubble and liquid bulk exists. For the two cavities condition, the dimensionless intensity of the hydrodynamic interaction h/h_0 is proposed to estimate the intensity of the hydrodynamic interaction between bubbles (interaction 2). It is defined as the ratio of convective heat transfer coefficient in a certain $S/\overline{D_b}$ condition, h, to that in the single cavity condition, h_0. The comparisons of h/h_0 for different $S/\overline{D_b}$ and laser power Q_{laser} are shown in Fig. 5.

It can be found that the hydrodynamic interaction between two bubbles (interaction 2) is very weak for $S/\overline{D_b} > 3$, which is similar to that in the single cavity condition. With reducing $S/\overline{D_b}$, this kind of hydrodynamic interaction becomes obviously stronger.

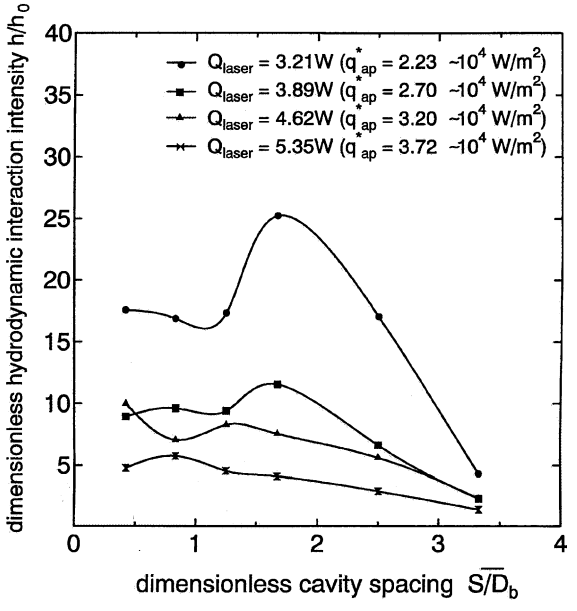

Fig. 5. Average dimensionless hydrodynamic interaction intensity h/h_0 for different $S/\overline{D_b}$ and laser power Q_{laser}.

3.2.2. Thermal interaction

During the bubble growth stage, heat is removed from the surface because of the liquid microlayer evaporation beneath the bubble and the microconvection around the bubble, which results in a cooled region around the bubble vicinity. This cooling effect not only inhibits the departure of the growing bubble [8], but also generates a negative effect on the adjacent bubble activity. Therefore, it can be imaged that with the strong effect of the thermal interaction, the nucleation site activity will be inhibited and the bubble departure frequency will become lower.

For the evaluation of the influence intensity of thermal interaction, the correlation coefficient between the temperature fluctuation at the cavity and that at a certain point j around the cavity is computed as

$$R_{cj} = \frac{C_{cj}}{r_c r_j} \tag{9}$$

where C_{cj} is the correlation function of the temperature fluctuation at the cavity c and the point j. It can be calculated as

$$C_{cj} = \frac{\sum_{i=1}^{n} (T_c^i - \overline{T_c})(T_j^i - \overline{T_j})}{n} \tag{10}$$

r is the standard deviation of the temperature fluctuation at a certain point and described as

$$r = \sqrt{\frac{\sum_{i=1}^{n} (T^i - \overline{T})^2}{n}} \tag{11}$$

Because the two cavities are symmetric with respect to the centerline of the surface, the temperature fluctuation of the points on the left part of the surface is correlated to that of the left cavity; so is the right part. The correlation coefficients of the temperature fluctuation are shown in Fig. 6.

Fig. 6 demonstrates that the thermal interaction between nucleation sites and heated wall (interaction 3) always has strong influence for all the $S/\overline{D_b}$ conditions because the correlation coefficients are high among a certain region around the cavities, which is similar to the single cavity condition (see Fig. 6(f)). For $S/\overline{D_b} > 2$, however, there is almost no thermal interaction between two cavities (interaction 4) because the correlation coefficients reach the minimum values within the center region between the two cavities (see Fig. 6(d) and (e)). With decreasing $S/\overline{D_b}$, the correlation coefficients in the central region become much higher, which states that the effect of interaction 4 becomes increasingly stronger (shown in Fig. 6(a)–(c)).

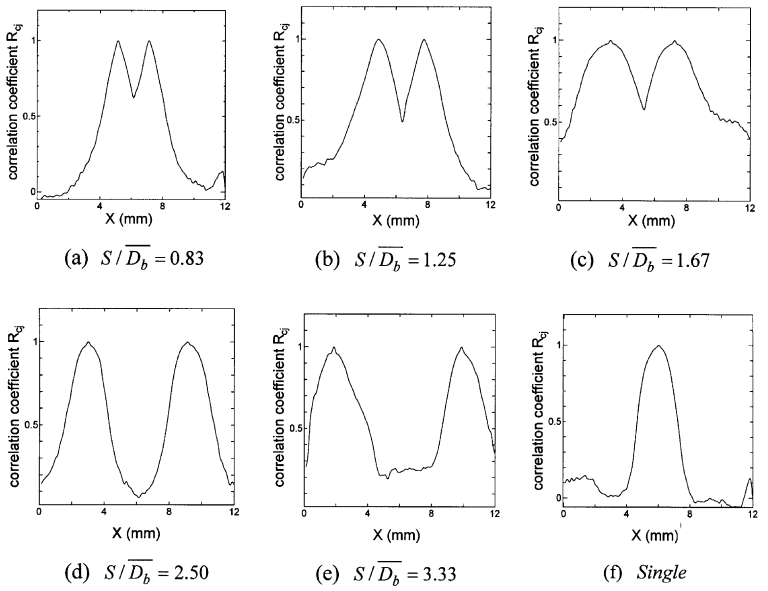

Fig. 6. Correlation coefficient of temperature fluctuation for different $S/\overline{D_b}$.

3.2.3. Bubble coalescence

Experimental results reveal that the bubble coalescences include two main kinds: coalescences far away from the surface and coalescences near the surface. Because the former one has very weak effect on the bubble growth and departure and the heat transfer of the surface [11], the present research only focuses on the bubble coalescences near the surface. From observation of the video, we can find that the coalescences near the surface can also be further classified into three types: vertical coalescence, horizontal coalescence and declining coalescence (shown in Fig. 7).

Vertical coalescence means that during the growth process of the following bubble, it contacts with the previous bubble and then seems to be pulled away and absorbed by the previous bubble within an extreme short time period. In Fig. 7(a), the small following bubble on the right side is absorbed by its previous bubble successively at the moments of $t = 195$ and 204 ms within several milliseconds. Horizontal coalescence is defined as that two growing adjacent bubbles contact with each other and then coalesce into one bigger bubble (Fig. 7(b) $t = 159$ and 60 ms). It seems that this coalesced bubble can reach force balance immediately through some deformation and then depart from the surface quickly (Fig. 7(b) $t = 161$ and 162 ms). Declining coalescence can be detected between a growing bubble on a nucleation site and a departed bubble over an adjacent nucleation site. In Fig. 7(c), the growing bubble on the left cavity contacts with the departed bubble over the right cavity at $t = 96$ ms. It is engulfed by the departed bubble instantly and a bigger coalesced bubble is formed at $t = 99$ ms. After that, the small growing bubbles on the right or left cavity are absorbed by this coalesced bubble consecutively at $t = 102$, 106 and 109 ms.

From above observation, it can be concluded that the bubble coalescences near the surface can promote the growing bubble to depart from the nucleation site. Consequently, the bubble departure frequency will become higher if the bubble coalescences near the surface occur.

On the other hand, the vertical coalescence can be observed for the conditions of single cavity and multiple cavities, while the horizontal and declining coalescences only arise in the condition of multiple cavities. Therefore, in the present analysis, only the occurrence frequencies of the horizontal and the declining coalescences are counted and compared, which is stated in Fig. 8. For $S/\overline{D_b} > 1.5$, there is no horizontal or declining coalescence between the adjacent bubbles. However, in the range of $S/\overline{D_b} \leqslant 1.5$, the frequency of the horizontal and the declining coalescences become increasingly higher. It can be predicted that for the region of $S/\overline{D_b} \leqslant 1.5$ the bubble growth and departure will be greatly promoted by the horizontal and the declining coalescences.

3.3. Mechanisms of nucleation site interaction—intensity, competition and dominance

From the above analysis, we can draw the conclusion that for studying the interaction mechanisms between two nucleation sites, there are three crucial effect factors: Ⓐ hydrodynamic interaction between bubbles; Ⓑ

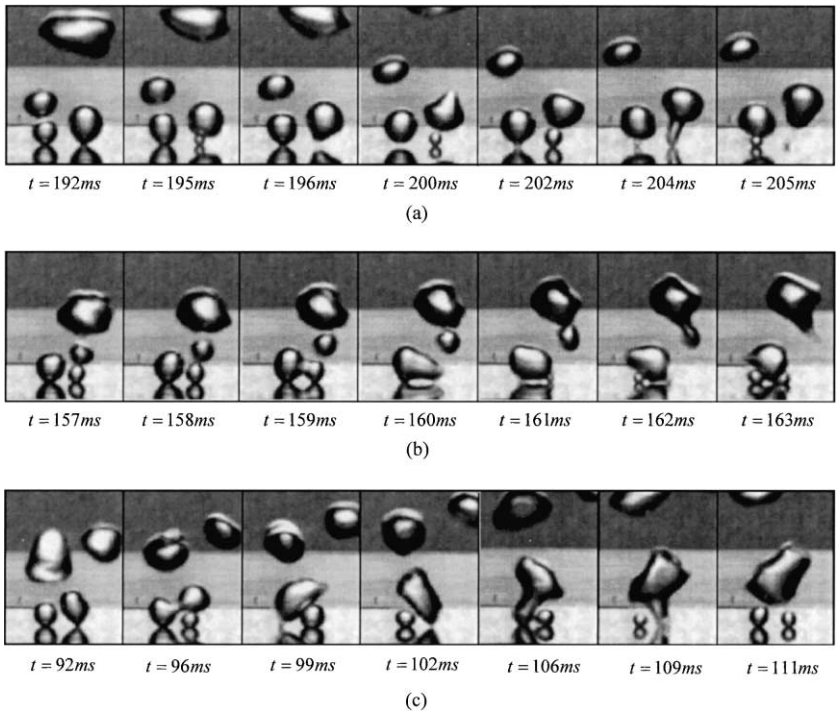

Fig. 7. Three types of bubble coalescence near the surface: (a) vertical coalescence; (b) horizontal coalescence; (c) declining coalescence.

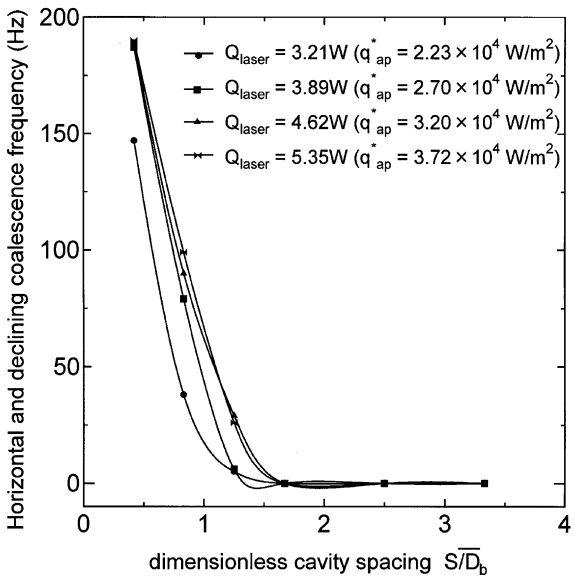

Fig. 8. Horizontal and declining coalescence frequency for different $S/\overline{D_b}$ and laser power Q_{laser}.

thermal interaction between nucleation sites; © horizontal and declining bubble coalescences.

The intensity regions of these three effect factors can be summarized in Table 1 and Fig. 9. For $S/\overline{D_b} > 3$, the influences of all these three effect factors are very weak and negligible, so that the bubble departure frequency is similar to that in the single cavity condition and this region is named 'I' region. However, in the region of $2 < S/\overline{D_b} \leqslant 3$, factor Ⓐ becomes stronger while the other two factors are still very weak, so that it is called 'H' region. As a result, the promotive effect becomes dominant and the average bubble departure frequency becomes higher than that in the 'I' region. With reducing $S/\overline{D_b}$, the influence of factor Ⓑ increases within the region of $1.5 < S/\overline{D_b} \leqslant 2$ ('H + T' region). Accordingly, factors Ⓐ and Ⓑ are conflicting with each other. In the present experiments, factor Ⓑ seems to be more significant than factor Ⓐ in this region. Especially as $q^*_{ap} = 2.23 \times 10^4$ W/m^2 (refer to Fig. 4), although the hydrodynamic interaction reaches the highest value, the average bubble departure frequency is still greatly damped by the occurrence of factor Ⓑ compared to the 'H' region. Consequently, inhibitive effect becomes dominant and the average bubble departure frequency becomes lower compared with the 'H' region. As for the condition of $S/\overline{D_b} \leqslant 1.5$, the influence of all the three factors become strong and compete simultaneously, which is consequently named 'H + T + C' region. However, it seems that the occurrence of factor © is very

Table 1
Influence intensity of three effect factors of nucleation site interaction for different $S/\overline{D_b}$

Main effect factors	$S/\overline{D_b}$				
	Effect on $\overline{f_d}$	$S/\overline{D_b} > 3$	$2 < S/\overline{D_b} \leqslant 3$	$1.5 < S/\overline{D_b} \leqslant 2$	$S/\overline{D_b} \leqslant 1.5$
Hydrodynamic interaction between bubbles (factor Ⓐ)	Promotive	×	○	○	○
Thermal interaction between nucleation sites (factor Ⓑ)	Inhibitive	×	×	○	○
Horizontal and declining coalescences (factor Ⓒ)	Promotive	×	×	×	○

×: negligible; ○: should be considered.

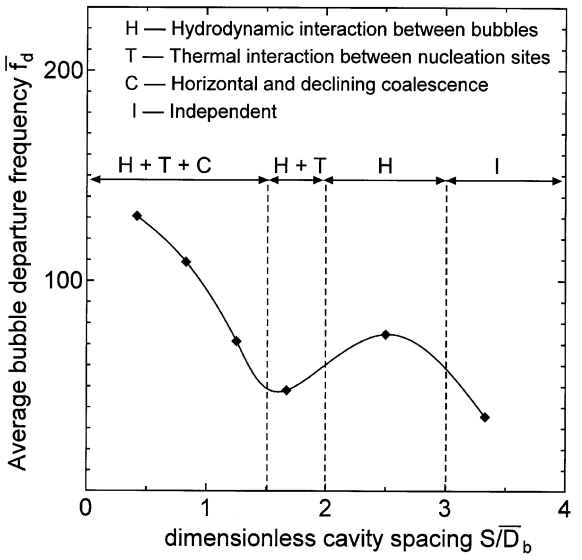

Fig. 9. Four regions of nucleation site interaction.

significant since it has positive effect not only on the bubble departure but also on the intensification of factor Ⓐ. These two positive factors become dominant in this region, which results in the much higher bubble departure frequency compared with the 'H + T' region.

In a word, the interaction of two nucleation sites depends on the intensity, competition and dominance of the three effect factors—hydrodynamic interaction between bubbles, thermal interaction between nucleation sites and horizontal and declining bubble coalescences.

4. Conclusions

The interactions mechanisms of two nucleation sites in pool boiling are comprehensively studied by a series of experiments on the artificial silicon surface. Three crucial effect factors of nucleation site interaction are found out: Ⓐ hydrodynamic interaction between bubbles; Ⓑ thermal interaction between nucleation sites; Ⓒ horizontal and declining bubble coalescences. The interaction between two nucleation sites relies on the intensity, competition and dominance relation of these three factors. Four different interaction regions are concluded: 'I' region ($S/\overline{D_b} > 3$), 'H' region ($2 < S/\overline{D_b} \leqslant 3$), 'H + T' region ($1.5 < S/\overline{D_b} \leqslant 2$) and 'H + T + C' region ($S/\overline{D_b} \leqslant 1.5$). In 'I' region, the influences of all the three factors are negligible, so the two artificial cavities are independent and the average bubble departure frequency is similar to that of the single cavity condition. For 'H' region, the intense influence of factor Ⓐ leads to the higher bubble departure frequency compared with the 'I' region. Within the 'H + T' region, factors Ⓐ and Ⓑ both become stronger and compete at the same time. The dominance of factor Ⓑ results in a lower bubble departure frequency. As for the 'H + T + C' region, the co-existence and competition relation of the three factors can be found. Because the promotive effect becomes absolutely dominant, the bubble departure frequency greatly increases again.

However, in the present experimental research, only the thin silicon surface is applied. It is known that the influence range of thermal interaction is also related to the thermal properties and thickness of the heated wall [6]. On the other hand, the hydrodynamic interaction can be also influenced by some other factors, such as the liquid properties, the subcooling, the system pressure and the like. Therefore, the competitive relation between the hydrodynamic interaction and the thermal interaction will become different for the different experimental conditions, which will result in the different tendency of the average bubble departure frequency. Although the presently observed trend of the average bubble departure frequency may be not reproducible for different experiments and the accurate delimitation of interaction regions also needs some further research, it is predictable that the proposed fundamental mechanisms of nucleation site interaction can be applied to analyze and demonstrate the experimental results even for different conditions, which is the key point of this paper.

Acknowledgements

The authors would like to express their gratitude to Prof. D.J. Lee of National Taiwan University and Prof. R. Mosdorf of Technical University of Bialystok, who have provided many suggestions to the present research.

The authors also thank their co-workers, Mr. Masanori Yokota, Mr. Koji Yasui and Mr. Masashi Tsushima for their efforts in doing the experiments.

References

[1] R.L. Judd, On nucleation site interaction, J. Heat Transfer 110 (1988) 475–478.
[2] V.V. Chekanov, Interaction of centers in nucleate boiling, Teplofzika Vysokikh Temperaur 15 (1977) 121–128.
[3] A. Calka, R.L. Judd, Some aspects of the interaction among nucleation sites during saturated nucleate boiling, Int. J. Heat Mass Transfer 28 (1985) 2331–2342.
[4] H. Gjerkeš, I. Golobič, Measurement of certain parameters influencing activity of nucleation sites in pool boiling, Exp. Thermal Fluid Sci. 25 (2002) 487–493.
[5] S.H. Bhavnani, G. Fournelle, R.C. Jaeger, Immersion-cooled heat sinks for electronics: insight form high-speed photography, IEEE Trans. Comp. Packag. Technol. 23 (2001) 166–176.
[6] D.B.R. Kenning, Y.Y. Yan, Pool boiling heat transfer on a thin plate: features revealed by liquid crystal thermography, Int. J. Heat Mass Transfer 39 (1996) 3117–3137.
[7] R.C. Lee, J.E. Nydhal, Numerical calculation of bubble growth in nucleate boiling from inception through departure, ASME J. Heat Transfer 111 (1989) 475–479.
[8] R. Mei, Vapor bubble growth in heterogeneous boiling—I. Formulation, Int. J. Heat Mass Transfer 38 (1995) 909–919.
[9] R. Mei, Vapor bubble growth in heterogeneous boiling—II. Growth rate and thermal fields, Int. J. Heat Mass Transfer 38 (1995) 921–934.
[10] L. Zhang, M. Shoji, A periodic bubble formation from a submerged orifice, Chem. Eng. Sci. 56 (2001) 5371–5381.
[11] J. Bonjour, M. Clausse, M. Lallemand, Experimental study of the coalescence phenomenon during nucleate pool boiling, Exp. Thermal Fluid Sci. 20 (2000) 180–187.